

# Effect of Process Parameters on Surface Quality for Wire Saw Cutting of Alumina Ceramic

Egemen TEOMETE<sup>1\*</sup>

<sup>1</sup> *Izmir Institute of Technology, Civil Engineering Department, Izmir, TURKEY.*

*Received: 31.01.2011 Accepted: 01.02.2011*

---

## ABSTRACT

Silicon wafers are sliced using wire saw in micro electronics and photo voltaic industries. Wire saw process occupies a great portion of silicon wafer production cost which affects the market directly. The process is also used to cut ceramics, concrete and rocks in civil engineering. The high cost of the process motivates researchers to develop models that will relate the process efficiency and quality with process parameters. In this study, an experimental parametric study was conducted to investigate the effect of process parameters on the wire bow angle, distributed wire load and surface roughness in wire saw cutting of alumina ceramic. The material removal and surface damage formation mechanisms are identified. Process design recommendations for increasing efficiency of the process while keeping the surface roughness constant, are presented. The surface roughness increases with increasing feed rate, decreases with wire speed and is independent of wire tension. The material is removed by trans-granular failure of the grains while inter-granular fractures of the grains affect the surface quality.

**Key Words:** *wire saw, ductile regime machining, surface roughness, ceramic.*

---

## 1. INTRODUCTION

Almost all kinds of brittle materials (including ceramics, concrete and rocks) and wood can be cut using wire saw with low surface damage [1-3]. The advantages of wire saw over inner diameter saw are less wafer surface damage, lower kerf loss and the ability to cut higher diameter wafers [1]. Wire saw process consists almost 30% of silicon wafer production cost which affects the market directly. The high cost of the process motivates researchers to develop models that will relate the process efficiency and quality with process parameters [4]. Bhagavat et al. [5] studied hydrodynamic film properties coupling Reynold's equation of hydrodynamics with elasticity equation of wire. Liu et al. [6] investigated the material removal mechanism of bead impregnated wire

saw cutting of marble and granite. Vibration characteristics of wire were investigated with respect to process parameters using finite element method [1, 7, 8]. Clark et al. worked on process monitoring of wire saw process for forces, wire speed, feed rate, wire bow and wire tension [9]. Wire life was investigated in cutting foam ceramics of silica-fused silicon carbide, transformation toughened zirconia, zirconia toughened alumina [2]. Surface and subsurface damage were related to wire speed, rocking frequency and down feed rate in a parametric study of wire saw cutting of silicon carbide ceramic by Hardin et al. [10]. Meng et al. [11] worked on closed loop fixed wire saw cutting of alumina and TiC ceramics. Direction of approach was determined for three

---

\*Corresponding author, e-mail: eteomete@gmail.com

most commonly sliced orientations of silicon by Bhagavat and Kao [12].

In this study, an experimental parametric study was conducted to investigate the effect of process parameters on the wire bow angle, distributed wire load and surface roughness in wire saw cutting of 99% purity alumina ceramic. Process design recommendations are presented for increasing efficiency of the process while keeping the surface roughness constant.

## 2. EXPERIMENTAL

A spool-to-spool wire saw machine (Millennium model, produced by Diamond Wire Technology in Colorado, Springs) was used in the experiments. The machine was controlled by wire speed, feed rate, wire tension and cut length of the wire. The cut length of the wire is the length which is translated to the take-up spool at each wire reversal. The cut length was set to 300 ft (91.4m) for all experiments.

During the cutting tests, coolant having water to lubricant Sawzit (product of Synthetic Lubricants Inc.) ratio of 50/1 was used. A diamond impregnated wire which had a diameter of 296  $\mu\text{m}$ , grit size of 66  $\mu\text{m}$  was used for the tests.

Alumina ceramic samples having 99% purity with mechanical properties presented in Table 1 were cut. The cut length of the samples were between  $L_o = 15\text{--}20$  mm and the samples' height were  $H_s = 7.1$  mm. The process parameters are presented in Table 2. The values used for process parameters are typical for fixed abrasive wire saw process and similar values were used by other researchers [2,9,15]. These process parameters are defined in Figure 1.

A Kodak digital camera of  $2856 \times 2142$  pixels was used to measure the wire bow angle. During the tests, images of wire and sample were captured. The images were

processed using Image Processing Toolbox of Matlab (Mathworks) to obtain the wire bow. An average of ten to fifteen images having steady wire bow was attained as the wire bow of the test.

An optical non-contact profilometer Zygo New View 6000 was used to obtain the surface roughness. The vertical resolution of the profilometer was 3 nm, the resolution on the horizontal plane was 1.1  $\mu\text{m}$ . Field of view of  $0.7 \times 0.53$  mm was obtained by 10x lens. Stitch measurements were applied on the left-middle-right of the cut surface in the direction of the wire feed, each having a dimension of  $0.7 \times 3$  mm. A high pass filter was applied to remove the surface waviness. The average of three measurements was attained as surface roughness of the test.

The cut surface topology was captured using scanning electron microscope (SEM) JEOL JSM-606LV. The SEM images were taken from the lower half of the surface where steady state wire bow was obtained.

Table 1. Mechanical properties of the 99% purity alumina ceramic [13,14].

Tensile strength MPa	300
Poisson's ratio	0,22
Fracture toughness MPam <sup>0.5</sup>	4
Young's Modulus GPa	370
Hardness GPa	22

Table 2. Process parameters.

Wire speed m/s	1.3-1.8-2.95-3.5
Feed speed $\mu\text{m/s}$	5-6.35-9
Wire tension N	13.3-22.4-26.7

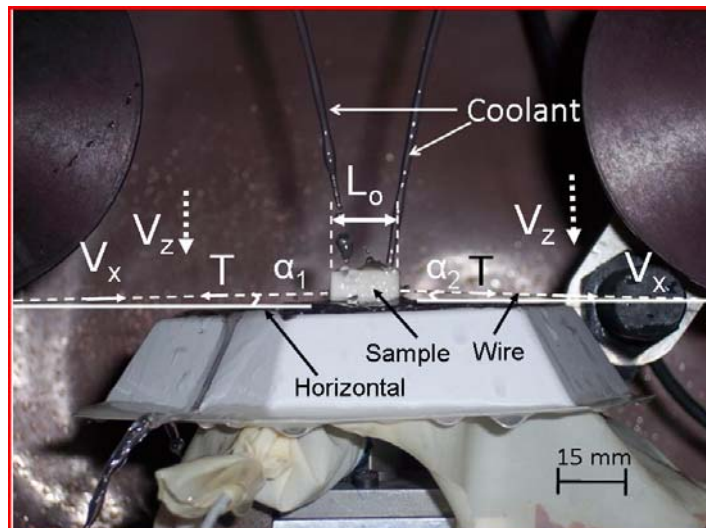


Figure 1. Typical cross section view of wire saw process. The process parameters wire speed  $V_x$ , feed rate  $V_z$  and wire tension  $T$  are defined on the figure.

**3. RESULTS AND DISCUSSION**

The scope of this study is to investigate the role of the wire saw process parameters on the quality of the produced surfaces. The variation of process outputs with process parameters are presented in this section.

In wire saw process, due to the wire tension  $T$  and wire bow  $\alpha$ , the wire applies a total force  $F_{zs}$  on the sample as in Figure 2. Using the equilibrium of forces principle, the sample applies an equal amount of force to the wire  $F_{zs}^w$ . The equilibrium of forces in the 2 direction in Figure 2 yields the total force acting on the sample by the wire,  $F_{zs}$ , in Eq. 1.

$$F_{zs}^w = F_{zs} = 2T \sin \alpha \tag{1}$$

The distributed force per length,  $w$ , acted by the wire on the sample can be obtained by dividing the total force,  $F_{zs}$ , by the cut length  $L_o$  as in Eq. 2. The distributed force on the sample is presented in Figure 2.

$$w = \frac{F_{zs}}{L_o} = \frac{2T \sin \alpha}{L_o} \tag{2}$$

The force per grit,  $F_{zg}$ , acted by a single abrasive grit on the sample, can be obtained by dividing the total force  $F_{zs}$  by the number of grits in the cut length, as in Eq. 3. The number of abrasive grits in the cut length can be calculated by  $N=L_o/L_g$ .  $L_o$  is the cut length of the sample (total contact length between the wire and the sample),  $L_g$  is the distance between abrasive grits.

$$F_{zg} = \frac{F_{zs}}{N} = \frac{2T \sin \alpha}{L_o} L_g \tag{3}$$

The experimental results in Figure 3 show that, for constant wire tension and feed speed, as wire speed increases, wire bow decreases. The decrease of wire bow

decreases the distributed force on the sample as seen in Figure 4. The decrease of wire bow also decreases the force per grit resulting in a lower surface roughness presented in Figure 5. For the same feed speed, as wire speed is increased, the depth of cut per abrasive grit decreases, resulting in lower force per grit and lower surface roughness as in Figure 5.

For constant wire speed and wire tension, experimental results show that the increase of feed speed  $V_z$  increases wire bow  $\alpha$  and the distributed load on the sample  $w$  as seen in Figures 6-7. The increase of wire bow increases force per grit which results in higher surface roughness as in Figure 8. The increase of feed speed increases depth of cut per abrasive grit, resulting in higher force per grit and higher surface roughness as seen in Figure 8.

The wire bow angle  $\alpha$  decreases with increasing tension  $T$  as in Figure 9. The increase of tension and decrease of  $\alpha$  leads to a constant distributed load due to Eq. 2 as seen in Figure 10. Similarly, increase of tension decreases wire bow and force on a single grit remains constant due to Eq. 3 which leads to a constant surface roughness with respect to tension as in Figure 11. For constant wire speed and feed, any change in wire tension is balanced by wire bow so that depth of cut per grit or force per grit does not change. Thus, surface roughness is independent of wire tension.

Ductile regime machining of brittle materials has been achieved by decreasing feed rate and increasing cutting speed which results in lower depth of cut per grit and lower force per grit [16, 17]. Similar phenomenon is observed in the SEM images of wire saw cut surfaces. Material removal is due to trans-granular deformation of the grains while inter-granular brittle fracture which leads to grain dislodgement is also effective in wire saw process as in Figure 12 (a-b).

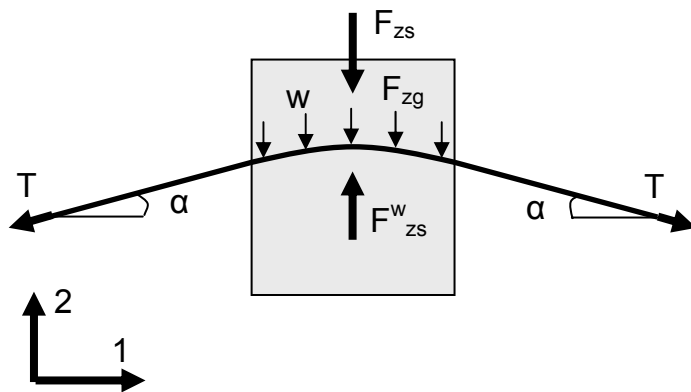


Figure 2. Cross section view of wire saw process. The total force acting on the sample by the wire  $F_{zs}$ ; the force acting on the wire by the sample  $F_{zs}^w$ ; the distributed force on the sample  $w$ ; the force per grit  $F_{zg}$  are presented.

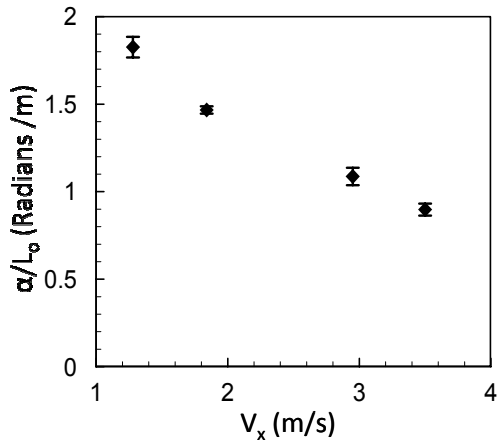


Figure 3. The variation of wire bow angle per unit cut length  $\alpha/L_0$  as a function of wire speed  $V_x$  ( $V_z = 5 \mu\text{m/sec}$ ,  $T = 13 \text{ N}$ ).

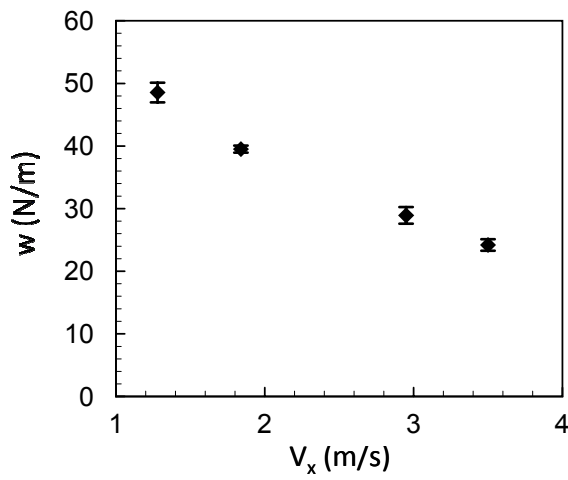


Figure 4. Variation of distributed load,  $w$  as a function of wire speed  $V_x$  ( $V_z = 5 \mu\text{m/sec}$ ,  $T = 13 \text{ N}$ ).

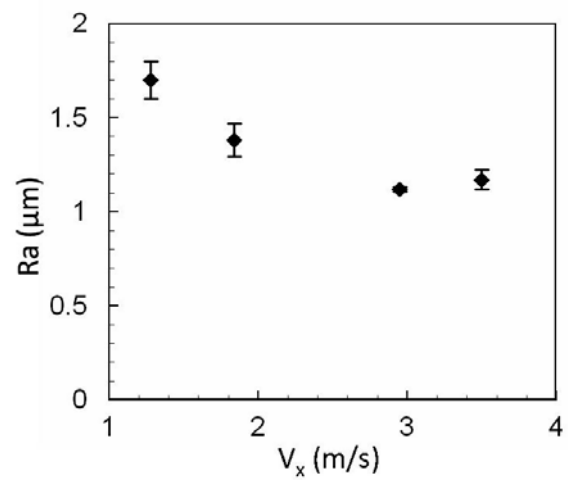


Figure 5. Variation of surface roughness as a function of  $V_x$  ( $V_z = 5 \mu\text{m/sec}$ ,  $T = 13 \text{ N}$ ).

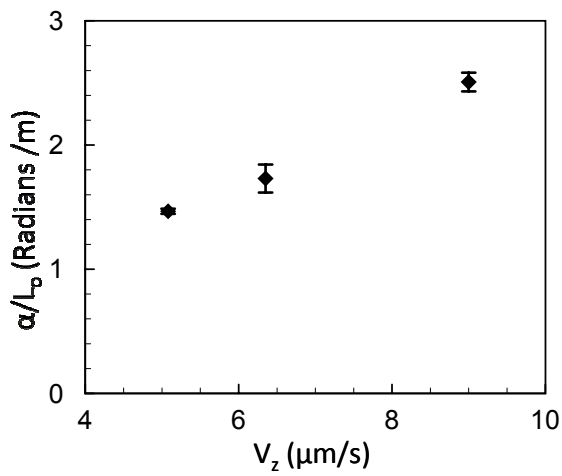


Figure 6. The variation of wire bow angle per unit cut length  $\alpha/L_0$  as a function of feed speed  $V_z$  ( $V_x = 1.8 \text{ m/sec}$ ,  $T = 13 \text{ N}$ ).

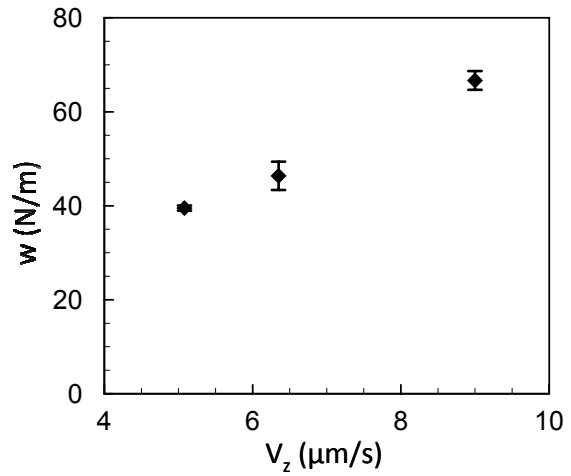


Figure 7. The variation of distributed load  $w$  as a function of feed speed  $V_z$  ( $V_x = 1.8 \text{ m/sec}$ ,  $T = 13 \text{ N}$ ).

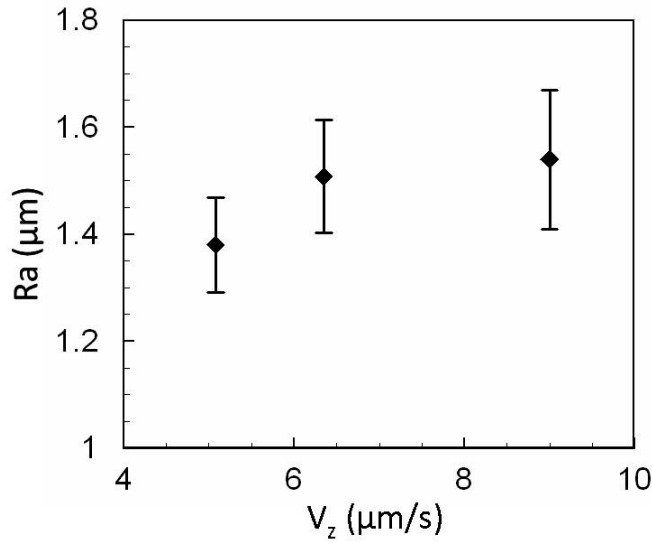


Figure 8. The variation of surface roughness as a function of feed speed  $V_z$  ( $V_x=1.8$  m/sec,  $T=13$  N).

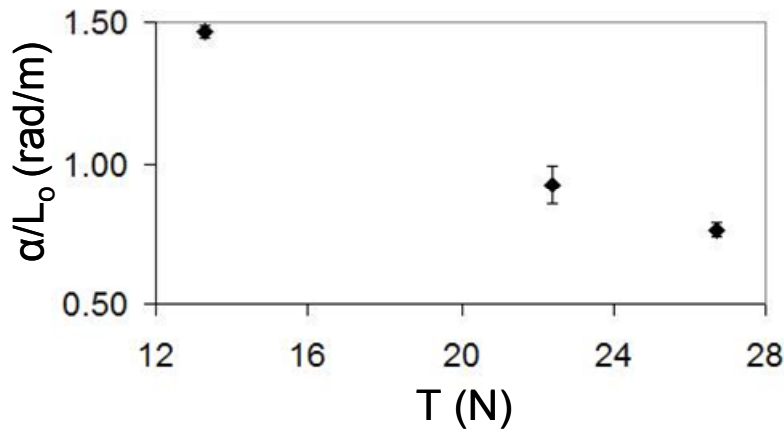


Figure 9. The variation of wire bow angle per unit cut length  $\alpha/L_0$  as a function of wire tension  $T$  ( $V_x=1.8$  m/sec,  $V_z= 5$   $\mu\text{m/sec}$ ).

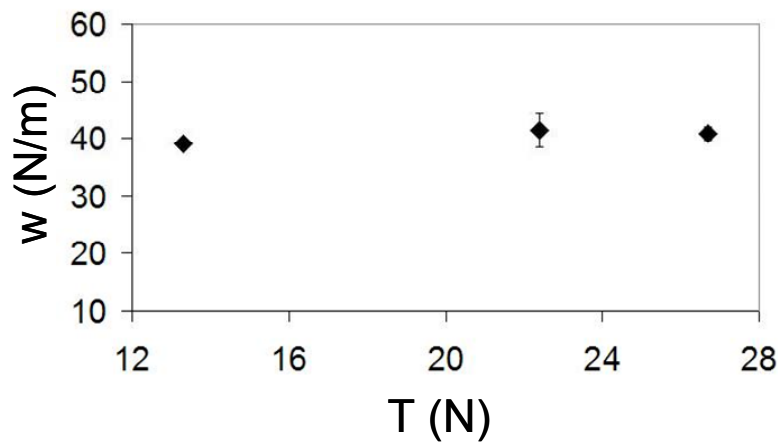


Figure 10. The variation of distributed load  $w$  as a function of wire tension  $T$  ( $V_x=1.8$  m/sec,  $V_z= 5$   $\mu\text{m/sec}$ ).

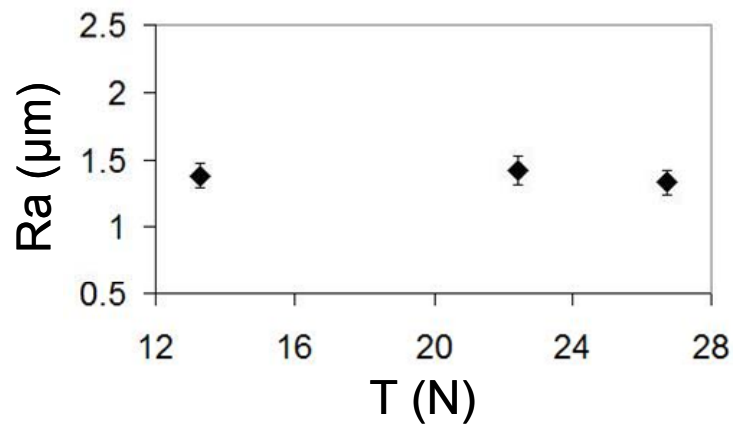


Figure 11. The variation of surface roughness as a function of wire tension  $T$  ( $V_x=1.8$  m/sec,  $V_z=5$   $\mu\text{m}/\text{sec}$ ).

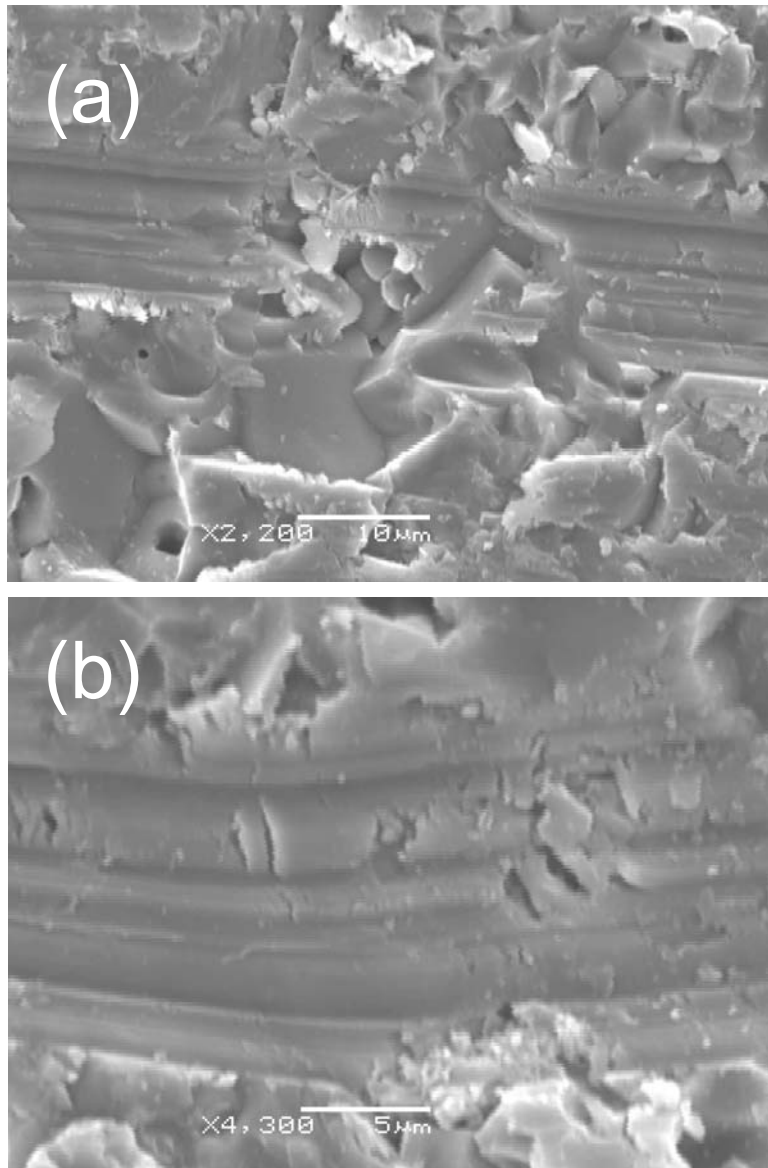


Figure 12. The SEM images of a wire saw cut surface ( $V_x=1.84$  m/sec,  $V_z=5$   $\mu\text{m}/\text{sec}$ ,  $T=13$  N). a) Ductile regime material removal and brittle fracture b) Ductile regime material removal.

#### 4. CONCLUSIONS

An experimental parametric study on wire saw process was conducted by varying wire speed, feed speed and wire tension which are process parameters. The variation of wire bow angle, distributed wire load and surface roughness with respect to process parameters was investigated experimentally.

Under constant feed speed and wire tension, increase of wire speed decreases wire bow angle. The decrease of wire bow angle decreases force per grit which decreases surface roughness. If the feed speed and wire tension are constant, increase of wire speed decreases depth of cut per abrasive grit, reducing force per grit and decreasing surface roughness.

With constant wire speed and tension, increase of feed rate increases wire bow resulting in an increase in force per grit and surface roughness. An increase in feed rate increases depth of cut per grit and force per grit which increases surface roughness.

Increase of wire tension decreases wire bow which leads to a constant load on the wire. The change in wire tension is balanced by change in wire bow and does not affect force per grit and surface roughness.

In order to increase the efficiency of the process without increasing the surface roughness, feed speed should be increased with wire speed.

The SEM images yields that dominant material removal mechanism is trans-granular failure of the grains while inter-granular failure leading to grain dislodgement decreases the surface quality.

#### ACKNOWLEDGEMENT

This work was supported by US-National Science Foundation NSF. This work is a part of the author's PhD study in Iowa State University. Author would like to thank to Iowa State University Aerospace Engineering and Mechanical Engineering Departments for their supports during this work.

#### REFERENCES

- [1] Hu, L., Kao, I., "Galerkin Based modal analysis on the vibration of wire-slurry system in wafer slicing using a wiresaw", *Journal of Sound and Vibration*, 283: 589-620 (2005).
- [2] Clark, W.I., Shih, A.J., Hardin, C.W., Lemaster, R.L., McSpadden, S.B., "Fixed abrasive diamond wire machining – Part II: experiment design and results", *International Journal of Machine Tools and Manufacture*, 43: 533-542(2003).
- [3] Ge, P.Q., Zhang, L., Gao, W., Liu, Z.C., "Development of endless diamond wiresaw and sawing experiments", *Materials Science Forum*, 471-472, 481-484(2004).
- [4] Moller, J.H., "Basic mechanisms and models of multi-wire sawing", *Advanced Engineering Materials*, 6-7, 501-513(2004).
- [5] Bhagavat, M., Prasad, V., Kao, I., "Elasto-hydrodynamic interaction in the free abrasive wafer slicing using a wiresaw: modeling and finite element analysis", *Transactions of ASME*, Tribology Division April, 122: 394-404(2000).
- [6] Liu, B.C., Zhang, Z.P., Sun, Y.H., "Sawing trajectory and mechanism of diamond wire saw", *Key Engineering Materials*, 259-260, 395-400(2004).
- [7] Wei, S., Kao, I., "Analysis of stiffness control and vibration of wire in wiresaw manufacturing process", *Proceeding of ASME*, Manufacturing Science and Engineering Division, 813-818(1998).
- [8] Wei, S., Kao, I., "Vibration analysis of wire and frequency response in the modern wire saw manufacturing process", *Journal of Sound and Vibration*, 231(5):1383-1395(2000).
- [9] Clark, W.I., Shih, A.J., Hardin, C.W., Lemaster, R.L., McSpadden, S.B., "Fixed abrasive diamond wire machining – Part I: process monitoring and wire tension force", *International Journal of Machine Tools and Manufacture*, 43: 523-532(2003).
- [10] Hardin, C.W., Qu, J., Shih, A.J., "Fixed abrasive diamond wire saw slicing of single-crystal silicon carbide wafers", *Materials and Manufacturing Processes*, 19(2): 355-367(2004).
- [11] Meng, J.F., Li, J.F., Ge, P.Q., Zhou, R., "Research on endless wire saw cutting of Al<sub>2</sub>O<sub>3</sub>/TiC Ceramics", *Key Engineering Materials*, 315-316, 571-574(2006).
- [12] Bhagavat, S., Kao, I., "Theoretical analysis on the effects of crystal anisotropy on wiresawing process and application to wafer slicing", *Machine Tool and Manufacture*, 46:531-541(2006).
- [13] Material Property Data, <http://www.matweb.com/index.aspx>, (accessed March 2008).
- [14] Cook, R.F., Pharr, G.M., "Direct observation and analysis of indentation cracking in glasses and ceramics", *Journal of American Ceramic Society*, 73(4): 787-817(1990).
- [15] Pei-Lum, T., Bo-Huei, Y., Hsing, L.C., "Study on thin diamond wire slicing with Taguchi method", *Materials Science Forum*, 505-507, 1219-1224(2006).
- [16] Yoshioka, J., Hashimoto, F., Miyashita, M., Kanai, A., Abo, T., Daito, M., "Ultraprecision grinding technology for brittle materials: application to surface and centerless grinding processes", Milton C. Shaw Grinding Symposium, R. Komanduri, D. Maas, eds. ASME Production Engineering Division, 16: 209-227(1985).
- [17] Bifano, T.G.; Dow, T.A.; Scattergood, R.O., "Ductile-regime grinding: a new technology for machining brittle materials", *Journal of Engineering for Industry*, 113: 184-189(1991).